VII International Conference on Particle-Based Methods
PARTICLES 2021
P. Wriggers, M. Bischoff, E. Oñate, A. Düster & T. Zohdi (Eds)

SIMULATION OF A CENTRIFUGAL PUMP BASED ON THE MESHLESS SOLVER

FENG WANG [*], ZHONGGUO SUN[†], ZIQI ZHOU, PEIDONG HAN, GUANG XI

[*] School of Energy and Power Engineering
Xi'an Jiaotong University
Xi'an 710049, China
e-mail: sun.zg@xjtu.edu.cn

Key words: MPS method, Centrifugal Pumps, Wall Boundary Conditions, Open Boundary conditions

Abstract. A three-dimensional full-scale centrifugal pump is simulated using the moving particle semi-implicit method (MPS). The genetic smooth wall boundary (GSW) is used and extended to 3D to deal with the complicated wall shape and thin-walled structure such as blades in turbo-machines. The non-surface detection technique (NSD) based on conceptual particles is combined with this wall model to avoid the loss of particle-number-density near wall boundaries. A local wall particle refinement method is developed. Fine particles and coarse particles are applied to curved surface and flat surface respectively so as to reduce the computational cost while maintain the high discretizing precision. The fully developed velocity inflow and pressure outflow boundary conditions are proposed. Two hydrostatic cases with complicated geometry are tested to verify the proposed models. This paper constructs a framework for the simulation of incompressible fluid machines, in which 3D complex revolving bodies can be integrally discretized and interactions between the stator and rotor can be integrally solved within a single coordinate. The results are compared with those of the fine volume method and good agreement is achieved. This paper provides a particle-based solver for incompressible fluid machinery and has the potential to study its inner flow with multiphase or phase change.

1. INTRODUCTION

The simulation of internal flow plays a vital role in the modern design process of fluid machinery. However, reproducing true flow conditions in up-to-date fluid machines has become increasingly difficult due to the complicated flow phenomena such as multiphase flow and phase change. These extreme conditions have imposed great challenges on the stability and performance of fluid machines.

Current numerical simulations dealing with flow inside fluid machines are mainly based on conventional mesh-based methods including the finite volume method (FVM) and finite difference method (FEM). Although relatively good results could be obtained, many assumptions and simplifications are involved.

Meshless methods including the moving particle implicit method(MPS) and smooth particle hydrodynamics method(SPH) are gradually showing advantages in numerically simulating flow fields in fluid machines[3]-[8], because these methods are able to integrally discretize and

integrally solve the flow field at interaction between the stator and rotor without the necessity to introduce other simplifications. Dynamic mesh is unnecessary and the simulation of large distortion can be easily achieved because the topology is not fixed.

Applicability of particle methods to a wide range of fluid machines has been proven by some scholars. Sun etc.[3] simulated a three-dimensional agitator with six straight blades and six guide blades using the MPS method. Wang etc.[18] apply the same scheme to studying mixing mechanism in a Y-type micromixer. Rahim[4] simulated the flow and mass transfer in a micro-pump mixer using the improved ISPH (incompressible smooth particle hydrodynamic) method. Kakuda[5] studied the formation of water ring in a liquid ring pump using the MPS method. Their results are compared with those calculated by the Petrov-Galerkin FE method and experiments.

Although the abovementioned researches have shown the ability of meshless methods in calculating fluid machines, studies about utilizing these methods to simulate a real centrifugal pump are still limited. Several difficulties including the construction of boundaries such as the wall boundary and open flow boundary may be responsible for it. Establishing a method to accurately discretizes complicated geometry is of great importance for simulating a centrifugal pump because there are many bowed and twisted surfaces in this fluid machine. In addition, a stable and accurate open boundary system including velocity inflow and pressure outflow plays a key role in precisely predicting the process of pressure increase.

The article is organized as follows: In section 2, the moving particle semi-implicit (MPS) is briefly introduced. In section 3, the GSW-NSD model and the open boundary conditions are demonstrated. In section 4, 3D cases are conducted to verify the effectiveness. In section 5, a real centrifugal pump is simulated using the above-mentioned models. Finally, some achievements and future work are summarized in section 6.

2. MOVING PARTICLE SEMI-IMPLICIT METHOD

The computational domain is discretized by a number of particles in MPS method. These particles are interacting with each other during the whole calculating process according to a kernel function (or weight function):

$$w(R)=\alpha\times\begin{cases}\dfrac{2}{3}-R^2+0.5R^3 & (R\le 1)\\ \dfrac{1}{6}\left(2-R\right)^3 & (1<R\le 2)\\ 0 & (R>2)\end{cases} \tag{1}$$

$$R=r/h$$

where $r=\left|\boldsymbol{r}_i-\boldsymbol{r}_j\right|$ is the distance between particle *i* and particle *j*, and r_e is the effective radius of the interaction zone. The gradient operator and Laplacian operator in governing equations can be obtained using space Taylor extension on each fluid particle.

$$\left\langle\nabla\varphi\right\rangle_i=\frac{d}{n_0}\sum_{j\ne i}\frac{\varphi_j+\varphi_i}{\left|\boldsymbol{r}_j-\boldsymbol{r}_i\right|^2}(\boldsymbol{r}_j-\boldsymbol{r}_i)w(\left|\boldsymbol{r}_j-\boldsymbol{r}_i\right|) \tag{2}$$

$$\left\langle \nabla^2 \varphi \right\rangle_i = \frac{2d}{\lambda n_0} \sum_{j \neq i} (\varphi_j - \varphi_i) w(|\boldsymbol{r}_j - \boldsymbol{r}_i|) \tag{3}$$

Where φ is an arbitrary scalar, d is the number of space dimensions, n_0 refers to the constant particle-number-density. The MPS method adopts the projection method to decouple pressure and velocity. The incompressible model consists of two steps, the deviation of the particle number density and the correction of it. The particle number density is defined as

$$\langle n \rangle_i = \sum_{j \neq i} w(|\boldsymbol{r}_j - \boldsymbol{r}_i|) \tag{4}$$

Single time step is divided into two parts. After the first explicit step, the particle number density would deviate from the ideal value and temporal parameters are calculated. Based on the abovementioned parameters, the Poisson equation is constructed to calculate pressure. The quasi-compressible pressure Poisson equation is adopted to reduce pressure oscillation[17], shown as Eq. (5).

$$\left\langle \nabla^2 p^{k+1} \right\rangle_i = (1-\gamma) \frac{\rho}{\Delta t} \nabla \cdot \boldsymbol{u}_i^* - \gamma \frac{\rho}{\Delta t^2} \frac{n^* - n^0}{n^0} \tag{5}$$

Finally, considering the pressure gradient which can be gained by Eq.(2), all the temporal parameters are corrected in the implicit step.

3. BOUNDARY CONDITIONS

3.1 GSW-NSD wall boundary

The shape of walls is represented by single layer wall particles, and the centers of these particles are accurately on the wall surface. A balance plane which is half of the particles' diameter away from walls is defined and fluid particles will be pushed against walls if their distance to walls is less than this parameter $0.5l_0$. $\boldsymbol{r_{ib}}$ and $\boldsymbol{dr}$ refer to the distances from fluid particles to the wall and to the balance plane respectively.

Pressure gradient is divided into two parts, the fluid part and the wall boundary part and interaction between the wall and nearby fluid particles is determined by the latter component.

$$\langle \nabla p \rangle_i = \langle \nabla p \rangle_{if} + \langle \nabla p \rangle_{ib} \tag{6}$$

The pressure gradient of wall part is obtained by Eq.(7). More deducting details can be found in the previous studies[1][17]

$$\langle \nabla p \rangle_{ib} = \frac{\rho |dr|}{\Delta t^2} \frac{\boldsymbol{r}_{ib}}{|\boldsymbol{r}_{ib}|} \tag{7}$$

Instead of involving $\boldsymbol{dr}$ into calculation, a particle bond model stemmed from the discretize element method (DEM) is introduced in the GSW model. This wall-particle contact model consists of one spring and one damping at both normal and tangible directions. The force $\boldsymbol{f}_i$ provided by the spring and damping prevents fluid particles from penetrating walls. The displacement of near-wall fluid particles can be calculated as follows

$$\left|dr\right| = f_i \Delta t^2 / m_i \tag{8}$$

Building a wall weight function is a common way to deal with this problem, as Eq.(9) shows.

$$n_{ib} = \sum w(\left|\boldsymbol{r_{ib}}\right|) \tag{9}$$

However, extra modifications are needed when irregular surfaces exist. Yijie Sun etc. [1]propose a general empirical function considering the right angle and round corner. These approaches can be useful and accurate in 2D cases, but for three dimensional cases, further discussion could be inevitable.

In this research, conceptual particles are used. As shown in Figure 1, conceptual particles automatically appear and elevate the particle number density to the normal level. The new particle number density $\langle n'' \rangle_i$ is defined as:

$$\langle n'' \rangle_i = \max(\langle n \rangle_i, \langle n' \rangle_i) \tag{10}$$

$$\langle n' \rangle_i = n^0 + \sum_{i,j \in fluid}^{Nr} [w(\left|\boldsymbol{r_{ij}}\right|) - w(l_0)] \tag{11}$$

The right second part of Eq.(11) is introduced to avoid particle cluster. The pressure Poisson equation needs to be accordingly modified as:

$$\frac{2d}{\lambda n^0}(\langle n'' \rangle_i^* P_i - \sum_{j \neq i}^{M} w(\boldsymbol{r_{ij}}) P_j) = \gamma \frac{\rho}{\Delta t^2} \frac{\langle n'' \rangle_i^* - n^0}{n^0} - (1-\gamma) \frac{\rho}{\Delta t} \nabla \cdot \boldsymbol{u}_i^* \tag{12}$$

M denotes the number of fluid particles j which are located in the searching area of particle i. Readers are recommended to refer to the previous study for more details[2].

3.2 Fully developed Inflow boundary

The basic concept of the fully developed inflow model lies on the moving inflow boundary approach[18]. An inflow region is defined and the velocity of particles in this area is fixed at a constant value, as shown in Figure 2.

In two dimensional cases, inlet cells are used to decide the moment of adding new particles, while inlet rings take place of these cells in 3D cases. To achieve a fully developed inflow condition, the first layer is divided into several rings and different levels of velocity are imposed on particles in different rings according to the theoretical velocity.

3.3 Pressure outflow boundary

A consistent and stable pressure outlet boundary condition based on the above-mentioned wall contact model is proposed. An outflow region is defined and each particle in this region will suffer a force from its corresponding virtual wall, as shown in Figure 2. The virtual wall moves with that outflow particle and keeps imposing a force on it. Outflow particles will be deleted when their pressure achieves specified value. At least three layers of outlet particles are needed in the outflow area to provide a complete kernel support for particles in the fluid domain.

4. VALIDATION

4.1 Hydrostatic cases with typical and complicated geometry

Figure 3 (a) presents the outline of the first case in which a mushroom shape is contained in a water tank. The other case, shown in Figure 3 (b) is a cone. The diameter of particles for water tanks is 2mm and most of curved surfaces in the mushroom and cone are discretized with 1.4mm particles, while the size of wall particles around irregular convex and concave parts can reach 1mm. The total numbers of the mushroom and cone cases are 31331 and 29504 respectively.

The pressure and velocity fields achieve a stable status after 0.3 seconds. Few pressure oscillations can be observed and the position of each fluid particle remains almost unchanged. Figure 4 (a) and (b) are the front views of these two cases. The outlines of both the mushroom and cone are clearly depicted. The free surfaces are very flat, which means the conceptual particles successfully compensate the particle-number-density loss. And irregular surfaces and the sharp vertex do not cause unphysical pressure perturbations.

4.2 Three-dimensional Poiseuille flow and divergence validation

Flow over a 3D tube is simulated in this regard to validate the accuracy, stability and convergence of the proposed models in 3D situation. The distance between two neighboring wall particles is 3mm. Figure 5 illustrates the geometry and wall particle model of the tube.

The fully developed inlet condition is utilized and the average inflow velocity is set as 6.25mm/s. Kinematic viscosity is 1×10^{-5} m^2/s. Four different sizes of fluid particles, ranging from 2.857mm to 5.263mm, are chosen to validate the convergence of our models. Transvers velocity of particles at the outlet section is measured and compared with theoretical results, as shown in Figure 6. It turns out that, with the increase of resolution, our results gradually converge to the theoretical results.

5. NUMERICAL RESEARCH ON THE CENTRIFUGAL PUMP WITH THE MPS METHOD

5.1 Generation of the wall particle model

As shown in Figure 7 and Figure 8, to reduce the total number of particles and hence improve calculating efficiency, the flat surfaces of the volute and impeller are represented by wall particles that are spaced 1mm apart. While a relatively small distance (0.6mm) between two wall particles are used for circular surfaces to avoid unphysical and discontinuous movement of fluid particles in these areas. The smallest interval (0.2mm) is applied to the volute tongue which is made up of the extremely complicated surfaces. Besides, as blades suffer severe pressure impact, this part would be discretized with more wall particles to prevent spurious pressure oscillations. With all the above-mentioned manipulations, the number of wall particles is 75732.

5.2 Solution parameter

There are 50825 fluid particles taking part in the simulation when the system achieves a stable status, and the diameter of these particles is 1.483 mm. A uniform initial fluid distribution,

shown in Figure 9, is obtained by gradually inputting fluid particles from the inlet tube to the empty wall model of that pump. Coordinates of these liquid particles will be extracted as initial arrangement.

All wetted surfaces are regarded as non-slip walls. Fully developed velocity inflow condition is imposed at the beginning of the inlet tube. Pressure outlet boundary condition is utilized and outlet pressure is 81000 Pa. The rotational speed of this impeller gradually increases from 0 to 2200 rpm to reduce pressure oscillation at startup stage. Inflow average velocity is determined according to the principle of hydraulic similitude during this period and eventually end up at 0.46356m/s. The density and dynamic viscosity of fluid are $1000kg/m^3$ and 1.0×10^{-4} m^2/s respectively.

5.3 Results and discussion

Our results are compared with those calculated by the finite volume method for the purpose of validation. Flow parameters and boundary conditions are set to the same. Unstructured mesh is used and the element size of the volute and impeller is 0.6mm. The inlet tube and outlet tube are extended to achieve fully-developed flow and avoid reverse flow respectively. The total number of cells is 9376719. Figure10 shows the pressure distribution on the middle plane of the volute calculated by two methods.

Some typical characteristics can be observed in the results of both methods. Pressure increases from the inlet center to the edge of the volute and is almost symmetric about Z axis. Pressure at the outlet is much bigger than that at the inlet, which means the basic function of a pump is achieved. Distributions of pressure calculated by two methods are in good agreement and present an obvious gradient change from the inlet center to the edge. A high-pressure region around the volute tongue is clearly captured.

To quantitatively compare results from two methods, four pressure monitoring points are set at the middle plane between the impeller and volute, as Figure 11 shows.

Pressure on these points calculated by two methods is shown in Figure 12, and it climbs with the increment of point serial numbers because the channel keeps expanding along the point-setting direction. The graph also illustrates the fluctuating amount of pressure at different points in MPS method, and the amplitude decreases along this direction for the reason that monitoring points become increasingly far away from the impeller as the point serial number grows, which leads to the decrease of the impeller's disturbance. The pressure values at each point are in good agreement between the MPS and FVM simulations and the maximum error is 5.64%.

6. CONCLUSION

This study constructs a totally Lagrangian framework in which the MPS method is applied to simulating a centrifugal pump. The state-of-the-art boundary conditions including the wall boundary and open boundaries are respectively improved and developed to fit into this framework.

The generic smoothed wall boundary[1] is used and extended to 3D situation. Conceptual particles[2] are generated to avoid the particle-number-density loss. Only single layer of wall particles is needed and because of this characteristic, it is possible to calculate the thin-walled structure such as impellers and volutes. A local wall-particle refinement technique is proposed. It turns out that this improved wall boundary condition is able to deal with complex 3D

geometry including twisted blades, extremely sharp vertexes and curves with variable curvature. By calculating two 3D hydrostatic cases with typical and complicated shape, we validate the GSW-NSD wall boundary. Open boundary conditions including fully developed velocity inflow and pressure outflow boundaries are proposed. Pressure outlet condition based on the moving virtual wall is able to provide a constant and steady pressure. The 3D Poiseuille case approves that the proposed open boundary conditions can obtain an accurate and stable velocity field.

Using the above-mentioned models, we successfully calculate a single-stage single-suction centrifugal pump. Initial fluid arrangement is obtained using the adaptability of particles and all the fluid particles closely adhere to the complicated surfaces, thereby perfectly presenting the shape. The pressure field is in good agreement with that computed by the FVM method and some qualitative features are accurately captured. Exact values of pressure at monitoring points are in accordance with those of FVM method.

This paper provides a new solver for the simulation of centrifugal pumps and experiences a whole numerical process including preprocess, calculation and postprocess. Other models such as multiphase and phase change models are expected to be added into this framework to investigate other key problems in the future.

REFERENCES

[1] Sun, Y.J., Xi, G., Sun, Z.G. A generic smoothed wall boundary in multi-resolution particle method for fluid–structure interaction problem. *Comput. Methods Appl. Mech. Engrg* (2021) **378**: 113-726.

[2] Chen, X., Xi, G., Sun, Z. G. Improving stability of MPS method by a computational scheme based on conceptual particles. *Comput. Methods Appl. Mech. Engrg* (2014) **278**: 254-271.

[3] Sun,Z.G., L.L., Xi G. Numerical simulation of the flow in straight blade agitator with the MPS method. *Int. J. Numer. Meth. Fluids* (2010) **67**: 1960-1972.

[4] Rahim S. Incompressible SPH modeling of rotary micropump mixers. *Int. J. of Comput. Methods* (2018) **15**: 191-207.

[5] Kakuda, K., Ushiyama, Y., Obara, S. Flow simulations in a liquid ring pump using a particle method. *Computer Modeling in Engineering & Sciences* (2010) **66**: 215-226.

[6] Zhe, J., Milos, S., Erwin, A.H. Numerical simulations of oil flow inside a gearbox by Smoothed Particle Hydrodynamics (SPH) method. *Tribology International* (2018) **127**: 47-58.

[7] Deng, X.Q., Wang, S.S., Wang, S.K. Lubrication mechanism in gearbox of high-speed railway trains. *Journal of Advanced Mechanical Design, Systems, and Manufacturing* (2020) **14**: 1-19.

[8] Guo, D., Chen, F.C., Liu, J. Numerical modeling of churning power loss of gear system based on moving particle method. *Tribology Transactions* (2020) **63**: 182-193.

[9] Zhang, T.G., Koshizuka, S., Murotani, K. Improvement of boundary conditions for non-planar boundaries represented by polygons with an initial particle arrangement technique. International *Journal of Computational Fluid Dynamics* (2016) **30**: 155-175.

[10] Zhang, T.G., Koshizuka, S., Murotani, K. Improvement of pressure distribution to arbitrary geometry with boundary condition represented by polygons in particle method. *Int. J.Numer. Meth. Engng* (2017) **112**: 685-710.

[11] Zhang, T.G., Koshizuka, S., Xuan, P. Enhancement of stabilization of MPS to arbitrary geometries with a generic wall boundary condition. *Computers and Fluids* (2019) **178**: 88-112.
[12] Matsunaga, T., Södersten A., Kazuya, S. Improved treatment of wall boundary conditions for a particle method with consistent spatial discretization. *Comput. Methods Appl. Mech. Engrg* (2020) **358**: 112-140.
[13] Wang, Z.D., Duan, G.T., Matsunaga, T. Consistent Robin boundary enforcement of particle method for heat transfer problem with arbitrary geometry. *International Journal of Heat and Mass Transfer* (2020) **157**: 119-139.
[14] Kazuya, S., Koshizuka, S., Kohei, M. Boundary conditions for simulating karman vortices using the MPS method. *Japan Society for Simulation Technology* (2015) **2**: 235-254.
[15] Tanaka, M., Cardosoa, R., Bahaia, H. Multi-resolution MPS method. *Journal of Computational Physics* (2018) **359**: 106-136.
[16] Kazuya, S., Issei, M., Masahiro, K. Improved pressure calculation for the moving particle semi-implicit method. *Comp. Part. Mech* (2015) **2**: 91-108.
[17] Tanaka, M., Masunaga, T. Stabilization and smoothing of pressure in MPS method by Quasi-Compressibility. *Journal of Computational Physics* (2010) **229**: 4279-4290.
[18] Wang F., Sun, Z.G., Liu, Q.X. Numerical analysis of flow field in the Y-type micromixer using MPS method. *Journal of Xi'an Jiaotong University* (2021) **55**: 5-14.
[19] Armaly, B.F., Dursts, F., Pereira, J.C.F., Schonung, B. Experimental and theoretical investigation of backward-facing step flow. *J. Fluid Mech* (1983) **127**: 473-496.
[20] Hu, F.Y., Wang Z.D., Tamai T., Koshizuka, S. Consistent inlet and outlet boundary conditions for particle methods. *Int. J. Numer. Meth. Fluids* (2020) **92**: 1-19.

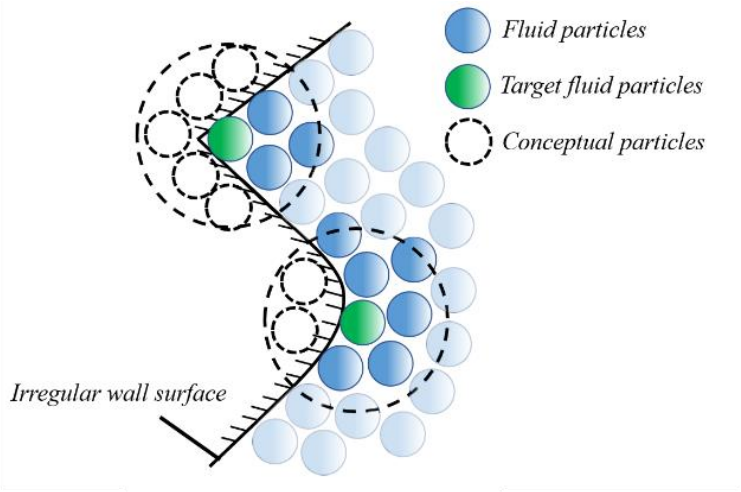

Figure 1: The GSW boundary with NSD technique

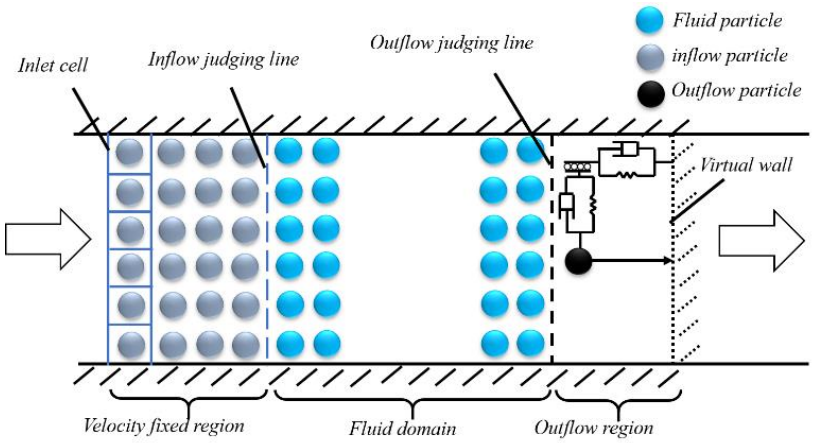

Figure 2: Description of the open boundary

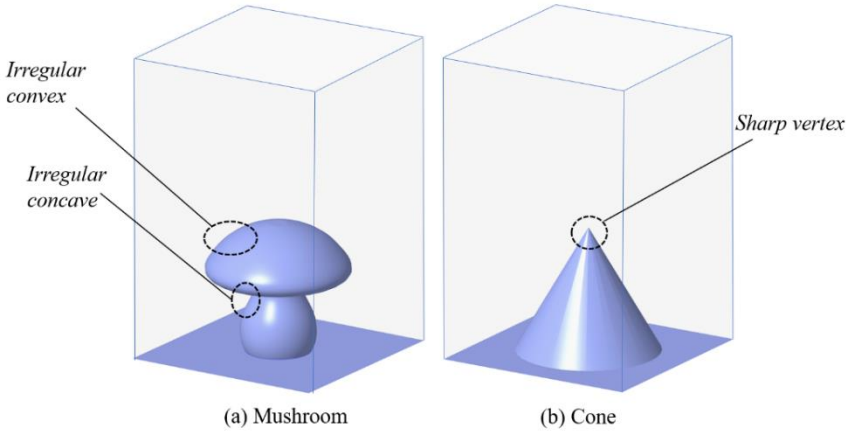

Figure 3: The geometry of two hydrostatic cases

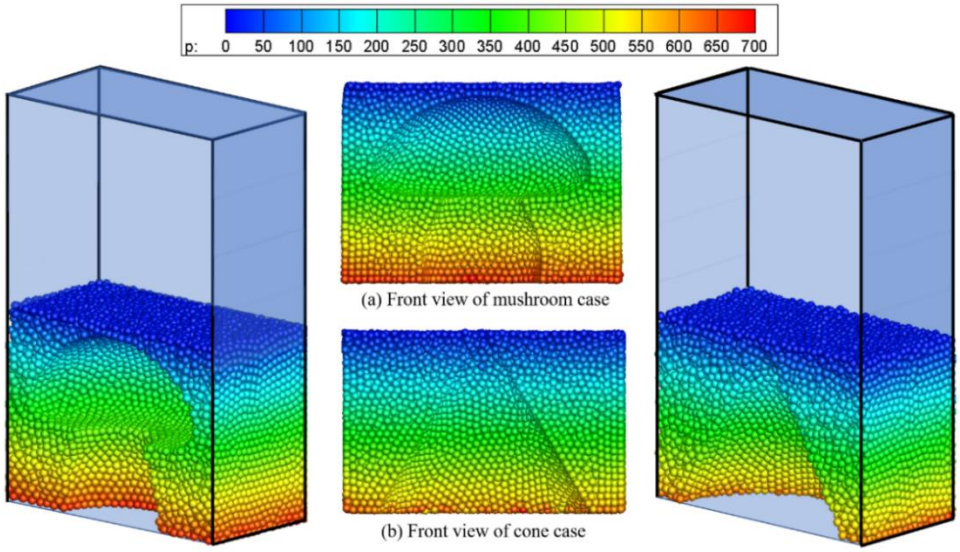

Figure 4: Pressure distribution and fluid particles' position of hydrostatic cases

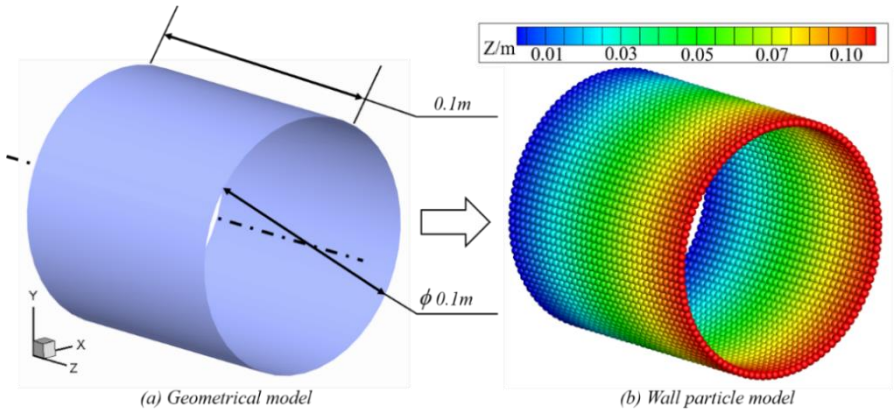

Figure 5: Discretion of the 3D tube

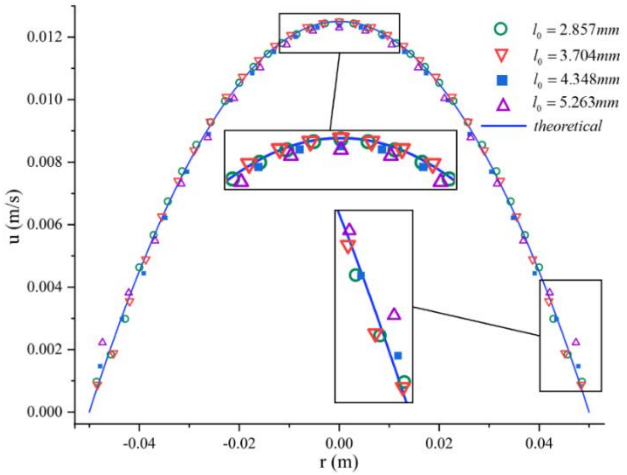

Figure 6: Comparison of MPS simulations at four resolutions with the analytical solution for Poiseuille flow

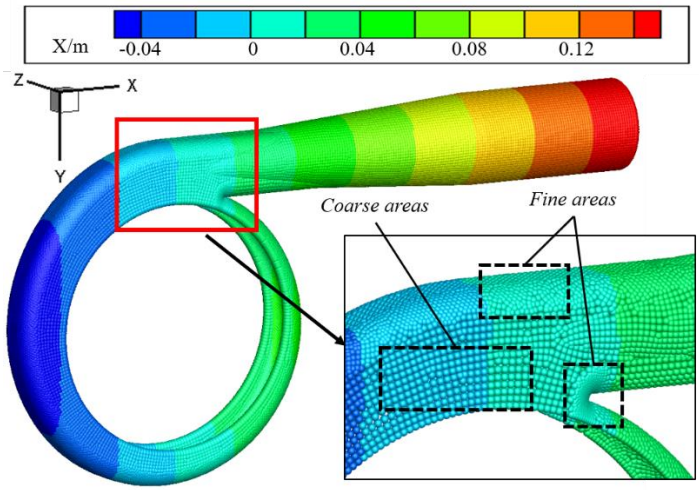

Figure 7: Discretization and local refinement of the volute

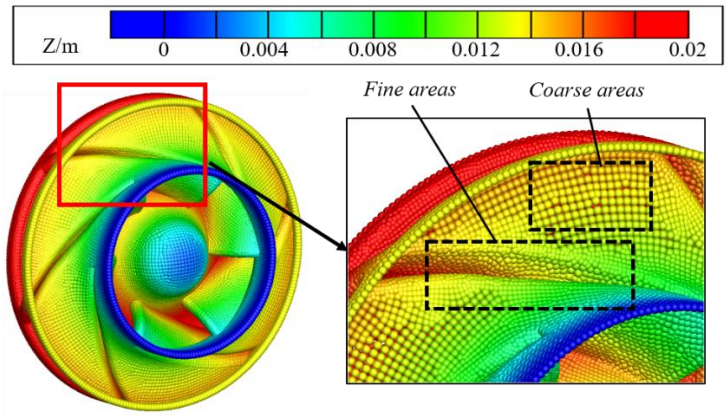

Figure 8: Discretization and local refinement of the volute

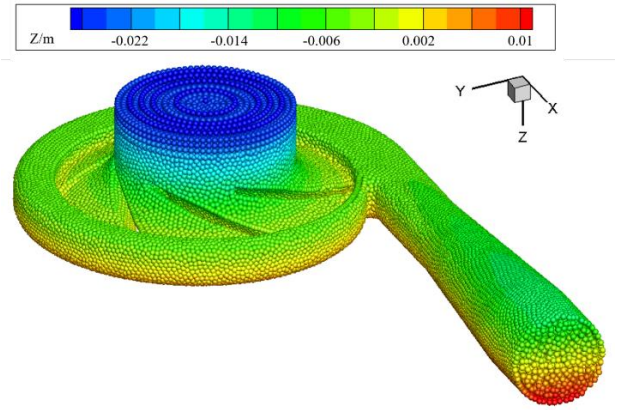

Figure 9: Initial distribution of fluid particles

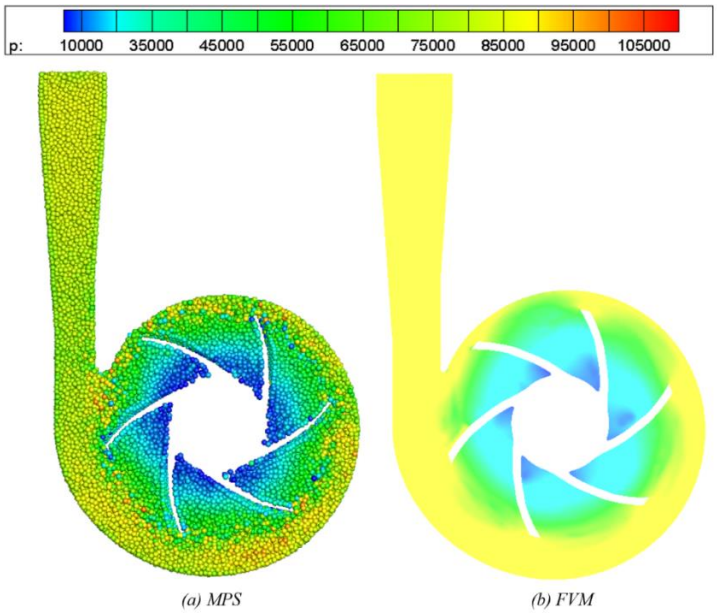

Figure10: Pressure distribution on middle plane by two methods

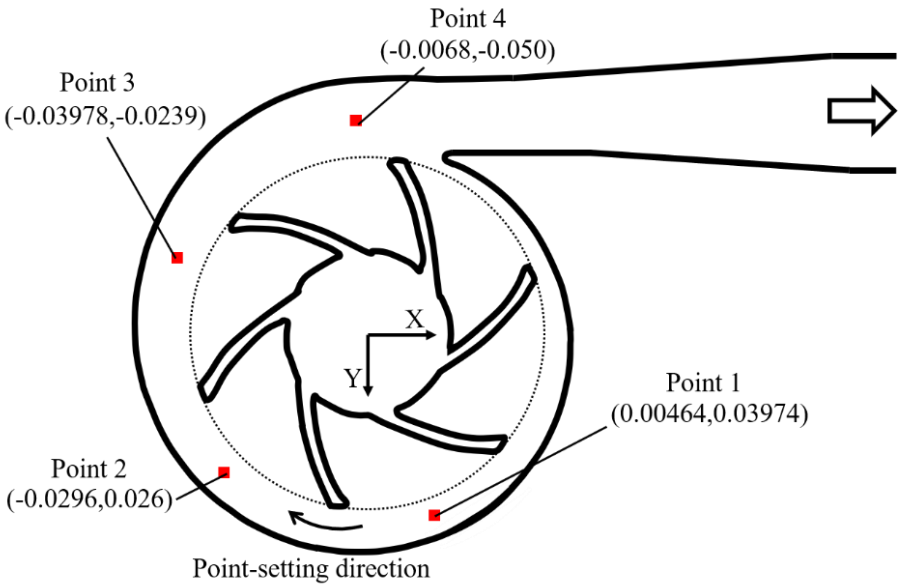

Figure 11: Position of four pressure monitoring points

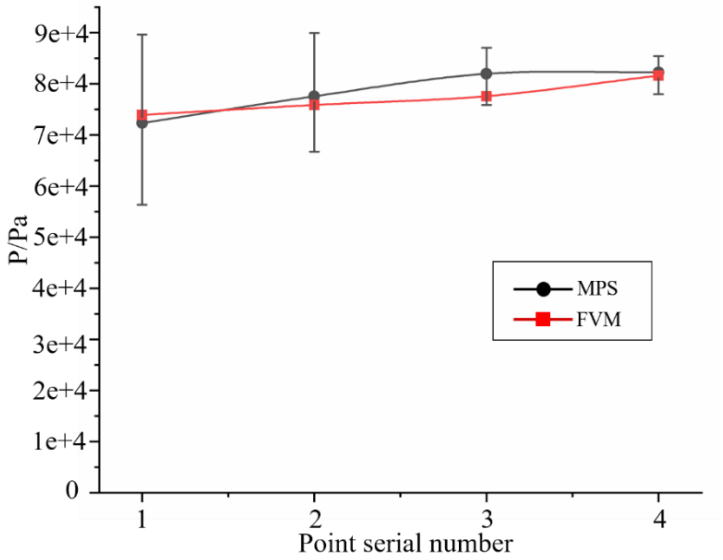

Figure 12: Pressure values at monitoring points from two methods